

# Structural Evaluation of Myofibrillar Proteins during Processing of Cantonese Sausage by Raman Spectroscopy

Weizheng Sun,<sup>†</sup> Qiangzhong Zhao,<sup>†</sup> Mouming Zhao,<sup>\*,†,§</sup> Bao Yang,<sup>‡</sup> Chun Cui,<sup>†</sup> and Jiaoyan Ren<sup>†</sup>

<sup>†</sup>College of Light Industry and Food Sciences, South China University of Technology, Guangzhou 510640, China

<sup>‡</sup>South China Botanical Garden, Chinese Academy of Sciences, Guangzhou 510650, China

<sup>§</sup>State Key Laboratory of Pulp and Paper Engineering, South China University of Technology, Guangzhou 510640, China

**ABSTRACT:** Structural changes of myofibrillar proteins from raw pork muscle and Cantonese sausage at different processing periods were elucidated using Raman spectroscopy. Fourier deconvolution combined with iterative curve fitting were used to analyze the amide I Raman band. Results from amide I, amide III, and C–C stretching vibrations in 890–1060 cm<sup>-1</sup> showed that  $\alpha$ -helix decreased accompanied by an increase in  $\beta$ -sheet structure during the first 18 h, and a rebuilding process of secondary structures was observed at the rest stage due to proteolysis. The hierarchical cluster analysis results of amide I and amide III confirmed this rebuilding process. Changes in a doublet near 850 and 830 cm<sup>-1</sup> suggested that some tyrosine residues became buried in a more hydrophobic environment due to intermolecular interactions. Raman spectra in the 2855–2940 cm<sup>-1</sup> region suggested that the environment of aliphatic side chains might have been changed during the final stage and further confirmed above rebuilding process.

**KEYWORDS:** Raman spectroscopy, myofibrillar proteins, structure, hierarchical cluster analysis, Cantonese sausage

## INTRODUCTION

Myofibrillar proteins, contributing to 55–65% of total muscle proteins, are the major protein fraction responsible for many physicochemical properties of muscle foods.<sup>1</sup> The physicochemical state of myofibrillar proteins affects the functionality of meat systems and plays a direct role in determining the quality and value of processed meat products.<sup>2</sup> The myofibrillar structure is a complex system with many protein–protein interactions.<sup>3</sup> Meat processing consists of a series of technological steps. Information concerning meat proteins and their behavior after slaughter and during aging is extensively documented.<sup>4,5</sup> Salting and heat treatment are two important steps of processed meat products. Thermally induced protein–protein aggregation is considered to be the key element to transform protein to a three-dimensional matrix during meat processing.<sup>6</sup> Recently, the evolution of myofibrillar protein of muscle has been mapped during salting and heat treatment.<sup>7–9</sup> They observed that structural evaluation of myofibrillar proteins was primarily affected by salting and cooking, resulting in protein functionalities changes, such as water binding ability.

The structural changes of protein can be examined at the molecular level by several methods such as circular dichroism, fluorescence spectroscopy, nuclear magnetic resonance (NMR), infrared absorption, and Raman spectroscopy. NMR methods mainly give detailed and specific information about peptides and proteins in solution and are limited to low molecular weight proteins.<sup>10</sup> Infrared spectroscopy methods present problems arising from the very strong infrared absorption of water at 1650 cm<sup>-1</sup>, in the middle of the amide I band.<sup>11</sup> Raman spectroscopy is a more suitable and direct technique that overcomes most of the above objections and can provide information on the secondary and tertiary structure of proteins in solid samples, like muscle food.<sup>12</sup> The Raman spectral assignments of proteins are usually based on model compounds such as amino acids or short peptides. Raman spectroscopy has been shown to be a useful tool to determine

structural changes that occur during processing of meat systems.<sup>9,11,13</sup> It has been used to study the structure of isolated meat proteins such as myosin.<sup>14,15</sup>

Cantonese sausage is a semidry sausage made in China, which has gained much popularity and acceptance over the world. Cantonese sausage is oven-dried at 42–50 °C for 3 days after salting. Salting and thermal treatment during meat processing strongly influence the protein changes. However, information concerning the structural changes of myofibrillar proteins during Cantonese sausage processing is still limited. Therefore, the objective of this work was to evaluate structural changes of myofibrillar proteins and their interactions by Raman spectroscopy at the molecular level.

## MATERIALS AND METHODS

**Samples and Materials.** Cantonese sausage samples (three replications) and raw pork muscle were collected from Jinrong Meat Products Co. Ltd. (Zhongshan, China). Raw muscle and back fat were obtained from a local commercial abattoir (Zhongshan, China), and the pigs were slaughtered at about 6 months of age following standard industrial procedures. Cantonese sausage was prepared according to the following formulation: lean pork (70 g), back fat (30 g), salt (3.5 g), sugar (12 g), wine (4 g), sodium nitrite (0.02 g), and water (20 g). These raw materials were mixed and stuffed into natural casings with a diameter of 37 mm and dried for 3 h at 50 °C with solar drying systems (Guangzhou Institute of Energy Conversion, Chinese Academy of Sciences, Guangzhou, China), followed by a reduction of temperature to the range of 45 °C, then dried for 21 h, and finally dried for 48 h at 42 °C. Samples (1000 g) were periodically taken at 0, 6, 18, 36, 54, and 72 h for each batch and kept at –18 °C for further use.

**Received:** June 27, 2011

**Accepted:** September 15, 2011

**Revised:** September 8, 2011

**Published:** September 15, 2011

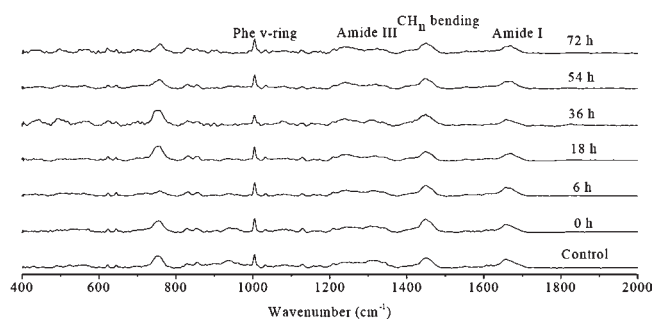


**Figure 1.** Raman spectra of myofibrillar proteins from raw muscle and Cantonese sausage at different processing periods in the 400–2000  $\text{cm}^{-1}$  region.

**Isolation of Myofibrillar Proteins.** Myofibrillar proteins were prepared according to the method of Martinaud et al.<sup>16</sup> Ten grams of Cantonese sausage was homogenized in 100 mL of sodium phosphate buffer solution (20 mM) at pH 6.5 containing 50 mM NaCl, 25 mM KCl, 3 mM  $\text{MgCl}_2$ , and 4 mM ethylenediaminetetraacetic acid, to which a protease inhibitor (1 mM PMSF) had been added, with an Ultra-Turrax homogenizer (Beijing Jingke Huarui Instrument Co. Ltd., Beijing, China) at 8000 rpm for 1 min in an ice bath. The homogenate was sieved through the sifter (mesh 250  $\mu\text{m}$ ), and collagen was eliminated by filtration on sifter. The extract was centrifuged at 2000g for 15 min at 4 °C. The pellet was washed twice with 100 mL of distilled water. The washed myofibril pellet was freeze-dried for Raman spectroscopy use.

The purity of myofibrillar proteins was assessed by sodium dodecyl sulfate–polyacrylamide gel electrophoresis according to the method of Flores et al.<sup>17</sup> The protein contents of myofibrillar proteins were 87–92%. The characteristic polypeptidic bands corresponding to myofibrils and to each major myofibrillar proteins were present in the gels. Results show that myofibril preparations were free of sarcoplasmic protein contamination (results not shown).

**Raman Spectroscopy.** Raman spectra with an excitation at 632.8 nm (laser He/Ne, less than 10mW on the sample) were obtained at room temperature, using a LABRAM-Aramis spectrometer (Horiba Jobin-Yvon, France). Spectral repeatability was smaller than 0.2  $\text{cm}^{-1}$ , and spectral resolution was better than 1  $\text{cm}^{-1}$ . Myofibrillar protein samples were placed on microscope slides. The laser was then focused on the samples. Raman spectra of at least three different positions were collected from 400 to 4000  $\text{cm}^{-1}$ . The spectral data from the scans of samples in the Raman spectrophotometer were baseline corrected and normalized according to the protein phenylalanine peak at 1003  $\pm$  1  $\text{cm}^{-1}$ . Protein secondary structures were determined as percentages of  $\alpha$ ,  $\beta$ , turns, and random conformations according to Susi and Byler.<sup>18</sup> The relative amounts of different protein secondary structures were determined from amide I spectra by computing the areas under the bands attributed to secondary structures. The areas of the bands were calculated by integration of the corresponding fitted band. Baseline correction, normalization, derivation, curve fitting, and area calculation were carried out by means of PeakFit Version 4.12 software (SPSS Inc., Chicago, IL), OPUS 6.5, and Origin 8.0 (OriginLab Corp., Northampton, MA) software.

**Statistical Analysis.** Statistical calculation and hierarchical cluster analysis were investigated using the statistical package SPSS 11.5 (SPSS Inc.). Data were subjected to analysis of variance (one-way ANOVA), and mean comparisons were carried out by least-squares difference.

## RESULTS AND DISCUSSION

Raman spectra of myofibrillar proteins from raw muscle and Cantonese sausage at different processing periods in the

400–2000  $\text{cm}^{-1}$  region are shown in Figure 1. The assignments of the Raman bands have been carried out according to literature references.<sup>11,12</sup> The frequency and intensity changes in the Raman bands were the main indicators of changes in the secondary protein structure and of variations in the local environments of myofibrillar proteins.

**Amide I.** *Analysis of Amide I Spectra Profile.* The most useful Raman bands to provide secondary structural information about proteins are the amide I (1600–1700  $\text{cm}^{-1}$ ) band, which mainly involves C=O stretching and, to a lesser degree, C–N stretching,  $\text{C}_\alpha$ –C–N bending, and N–H in-plane bending of peptide groups.<sup>11,12</sup> Susi and Byler<sup>18</sup> reported that Fourier deconvolution of the amide I Raman band combined with iterative curve fitting could yield useful quantitative conformation of protein. In this work, Fourier deconvolution and iterative curve fitting were used to analyze an amide I Raman band of myofibrillar proteins from raw muscle and Cantonese sausage at different processing periods. Deconvolved and curve-fitted amide I Raman bands of myofibrillar proteins are shown in Figure 2. For the raw myofibrillar proteins, the major feature of the amide I band was centered at 1657  $\text{cm}^{-1}$ , indicating a predominance of the  $\alpha$ -helical structure, and a small shoulder near 1680  $\text{cm}^{-1}$  suggested the minor contribution of  $\beta$ -sheet in the myofibrillar proteins. Salting (0 h) induced a trend toward uncoiling of helices, which was confirmed by the shift of the major band to 1660  $\text{cm}^{-1}$ . The obvious shoulder band near 1675–1680  $\text{cm}^{-1}$  assigned to the  $\beta$ -sheet structure was evident at the sixth hour. As processing proceeded, the band near 1675–1680  $\text{cm}^{-1}$  gradually became dominant except at the 36th hour. However, these samples differed in other minor features. For example, the spectra of the 54th and 72nd hours showed a minor band near 1656  $\text{cm}^{-1}$ . It was noteworthy that, at the 36th hour, the band near 1656  $\text{cm}^{-1}$  was higher than that near 1675  $\text{cm}^{-1}$ , indicating that the  $\alpha$ -helical structure increased.

The corresponding results of the curve-fitting analysis expressed as a function of percentage areas of main protein secondary structures are in Table 1. There was a decrease ( $p < 0.05$ ) in the  $\alpha$ -helix accompanied by an increase ( $p < 0.05$ ) in the  $\beta$ -sheet structure during 0–18 and 36–72 h. However, there is a tendency for the decrease ( $p < 0.05$ ) of the  $\beta$ -sheet content with simultaneous increase ( $p < 0.05$ ) of the  $\alpha$ -helix content during 18–36 h. These results were consistent with the amide I spectra changes (Figure 2).

Some authors have reported the changes in protein secondary structure upon addition of inorganic salts in isolated myosin solutions. Reduced  $\alpha$ -helix observed in myosin in the presence of inorganic salts such as  $\text{CaCl}_2$ ,  $\text{MgCl}_2$ , and LiBr can be explained by an increase in interchain hydrogen bonding.<sup>15</sup> Fourier transform infrared (FTIR) spectroscopic analysis of pork muscle, subjected to brine salting at different concentrations, has shown protein structural changes in terms of decreases in  $\alpha$ -helix content at a salt concentration higher than 3%.<sup>8</sup> Studies of heat-induced structural changes in meat myofibrillar proteins, determined by FTIR spectroscopy, had indicated an increase in  $\beta$ -sheet structure levels.<sup>7</sup> Herrero et al.<sup>9</sup> reported that the establishment of a stable gel network upon heating is closely linked to an increasing hydrogen-bonded  $\beta$ -sheet structure. Studies in roasted beef indicated that the  $\alpha$ -helical to  $\beta$ -sheet ratio is an important factor contributing to the shear force, tenderness, acceptability of texture, and overall acceptability of meat.<sup>19</sup> Moreover, Bouraoui, Nakai, and Li-Chan<sup>20</sup> reported that the structure change was possibly through intermolecular

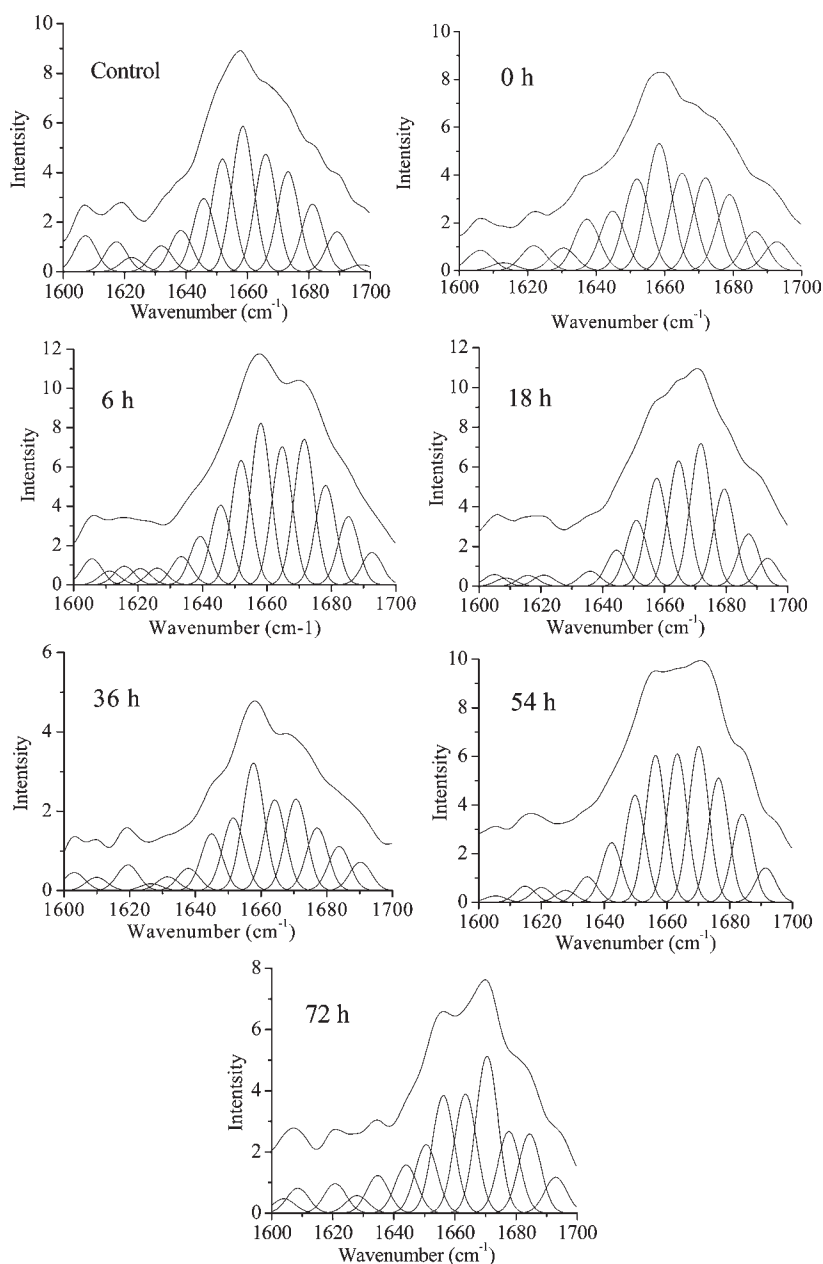


**Figure 2.** Deconvolved and curve-fitted Raman bands of amide I of myofibrillar proteins from raw muscle and Cantonese sausage at different processing periods.

interactions between exposed hydrophobic residues, which increased during cooking. In the present work, changes in amide I during 0–18 and 36–72 h could also be due to an unfolding of helical structures, followed by the formation of sheet structures. An increase in  $\alpha$ -helix accompanied by a decrease in  $\beta$ -sheet structure during 18–36 h might be due to proteolysis of Cantonese sausage, which involves the decrease of high molecular weight proteins and the formation of polypeptides and free amino acids.<sup>21</sup> Enzymatic hydrolysis of proteins, especially partial hydrolysis, is often employed to improve the functionalities of food proteins.<sup>22,23</sup> Such functionality changes were related to alterations in protein structure, including partial unfolding, altered isoelectric point, and increased hydrophobicity. These discrepancies between the 36th hour and the other periods might be due to changes of myofibrillar proteins composition due to proteolysis. Proteolysis

is an important biochemical behavior occurring during the processing of Cantonese sausage.<sup>24</sup> The appearance of bands with some vibration frequencies in the Raman spectra depends on the molecular geometry and the chemical composition of substance tested.<sup>12</sup> Proteolysis might lead to the myofibrillar proteins undergoing a rebuilding process of secondary structures. In addition, the structure of random and other types at the 36th hour increased as compared to the others, confirming this rebuilding process.

*Hierarchical Cluster Analysis of Amide I.* Multivariate statistical techniques are the right tools for viewing and analyzing a matrix of complex data. Hierarchical cluster analysis consists of mathematically treating each variable as a point in the multi-dimensional space described by the samples.<sup>25</sup> When a given sample is taken as a point in the space defined by the variables,

**Table 1. Determined Frequencies of Amide I Component Bands, Relative Assigned Structures, and Their Distributions for Secondary Structural Contents of Myofibrillar Proteins from Raw Muscle and Canteese Sausage at Different Processing Periods**

structure <sup>d</sup>	frequency (cm <sup>-1</sup> )/structure distribution (%)						
	control	0 h	6 h	18 h	36 h	54 h	72 h
amino acid side chains	1607 (4.46 ± 0.47 c) 1617 (3.71 ± 0.47 c) 1622 (1.76 ± 0.45 a) 1632 (3.19 ± 0.31 c) 1638 (5.11 ± 0.46 d) 1646 (9.02 ± 0.91 c) 1652 (13.88 ± 0.84 d) 1659 (17.91 ± 1.40 bc) 1666 (14.49 ± 1.84 ab) 1673 (12.34 ± 1.80 ab)	1607 (2.73 ± 0.43 b) 1613 (1.05 ± 0.19 a) 1622 (3.33 ± 0.32 b) 1630 (3.03 ± 0.38 c) 1637 (6.88 ± 0.44 e) 1645 (7.97 ± 1.20 bc) 1652 (12.26 ± 1.81 cd) 1658 (16.99 ± 0.99 bc) 1665 (13.01 ± 1.76 a) 1672 (13.50 ± 1.03 abc)	1606 (2.56 ± 0.41 b) 1621 (1.59 ± 0.31 a) 1626 (1.64 ± 0.38 a) 1633 (3.77 ± 0.40 c) 1639 (5.41 ± 0.81 d) 1646 (7.83 ± 0.89 bc) 1652 (12.24 ± 1.99 cd) 1658 (15.88 ± 1.75 ab) 1665 (13.61 ± 1.75 a) 1672 (15.81 ± 1.91 c)	1605 (1.65 ± 0.51 a) 1609 (1.15 ± 0.17 a) 1616 (1.51 ± 0.48 a) 1621 (1.57 ± 0.39 ab) 1636 (2.10 ± 0.27 a) 1645 (5.04 ± 0.89 a) 1651 (9.25 ± 0.83 ab) 1657 (15.18 ± 1.53 ab) 1665 (17.61 ± 1.47 b) 1672 (20.04 ± 1.48 e)	1604 (2.69 ± 0.33 b) 1619 (3.82 ± 0.31 c) 1627 (1.02 ± 0.18 a) 1632 (2.04 ± 0.46 b) 1638 (3.30 ± 0.38 bc) 1645 (8.44 ± 0.99 c) 1652 (10.83 ± 1.54 abc) 1658 (18.99 ± 1.41 c) 1664 (14.01 ± 1.48 a) 1671 (14.13 ± 1.39 abc)	1606 (0.68 ± 0.18 a) 1615 (1.69 ± 0.32 a) 1620 (1.58 ± 0.25 a) 1628 (1.26 ± 0.33 a) 1635 (2.71 ± 0.43 ab) 1642 (6.35 ± 0.91 a) 1650 (11.42 ± 1.52 bcd) 1656 (15.65 ± 1.52 ab) 1663 (15.81 ± 1.43 ab) 1670 (16.61 ± 2.27 cd)	1605 (1.50 ± 0.31 a) 1609 (2.55 ± 0.44 b) 1621 (3.11 ± 0.29 b) 1628 (2.15 ± 0.32 b) 1635 (4.10 ± 0.37 c) 1644 (5.90 ± 0.51 a) 1651 (8.40 ± 0.58 a) 1656 (14.41 ± 1.73 a) 1663 (14.57 ± 0.68 a) 1670 (19.20 ± 1.92 de)
β-sheet							
turn							
random							
α-helix							
β-sheet							
turn							
α-helix							
β-sheet							
turn							
random							
other							

<sup>a</sup>Susi and Byler<sup>18</sup> and Iconomidou et al.<sup>32</sup>. α-Helix, band at 1650–1652 cm<sup>-1</sup>; β-sheet, bands at 1620–1627, 1628–1632, 1663–1665, and 1670–1673 cm<sup>-1</sup>; turns, band at 1635–1639 cm<sup>-1</sup>; random coil, band at 1642–1646 cm<sup>-1</sup>; other (amino acid side chains), bands at 1604–1607 and 1609–1619 cm<sup>-1</sup>; 6 h, 1621 cm<sup>-1</sup> attributed to amino acid side chains; and 18 h, 1616 cm<sup>-1</sup> attributed to β-sheet.



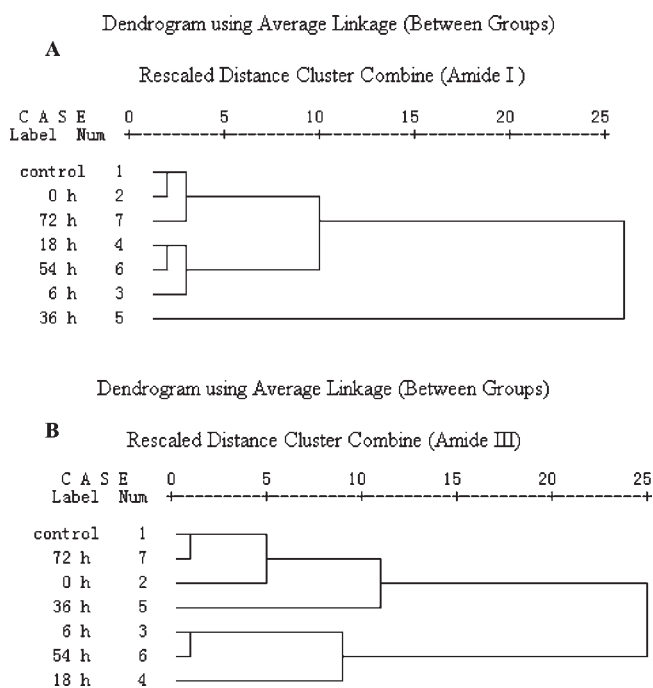


**Figure 3.** Dendrograms of amides I ( $1600\text{--}1700\text{ cm}^{-1}$ ) and III ( $1220\text{--}1275\text{ cm}^{-1}$ ) of myofibrillar proteins from raw muscle and Cantonese sausage at different processing periods (A, amide I; B, amide III).

one can calculate the distance between this point and the other points, thereby establishing a matrix that describes the proximity between all of the samples studied. Thus, hierarchical cluster analysis is a simple way of grouping the samples studied through similarity to evaluate the influence of salting and processing on the structural changes of myofibrillar proteins of Cantonese sausage.

Results of hierarchical cluster analysis for amide I are present in Figure 3A. Three clusters were observed in the dendrogram. The first cluster consisted of the three samples of control, zero hour, and 72nd hour. The second cluster consisted of the three samples of the 6th, 18th, and 54th hours. The third cluster is the sample of the 36th hour. It could be seen that control and zeroth hour were clustered together first, and then, the 18th and 54th hours were clustered. These indicated that they had a great proximity. Then, the 72nd and 6th hours were successively clustered into the group of control and 54th hour, respectively. The sample of the 36th hour was separated individually in the dendrogram from the other samples. These results further confirmed the rebuilding process of myofibrillar proteins during the processing of Cantonese sausage.

**Amide III.** *Analysis of Amide III Spectra Profile.* The  $\text{--CO--NH--}$  amide or peptide bond has several distinct vibrational modes, with the amide I band near  $1650\text{ cm}^{-1}$  and the amide III band near  $1250\text{ cm}^{-1}$ . The exact location of these bands depends on the secondary structure of the polypeptide chain. Because of possible overlap of bands from miscellaneous C–H bending and aromatic ring vibrations in the amide III region, it is recommended that both regions are analyzed to obtain a more reliable interpretation of the changes in the secondary structure of proteins.<sup>11,12</sup>

This spectroscopic Raman band of amide III involves C–N stretching and N–H in-plane bending vibrations of the peptide bond as well as contributions from C $\alpha$ –C stretching and C=O

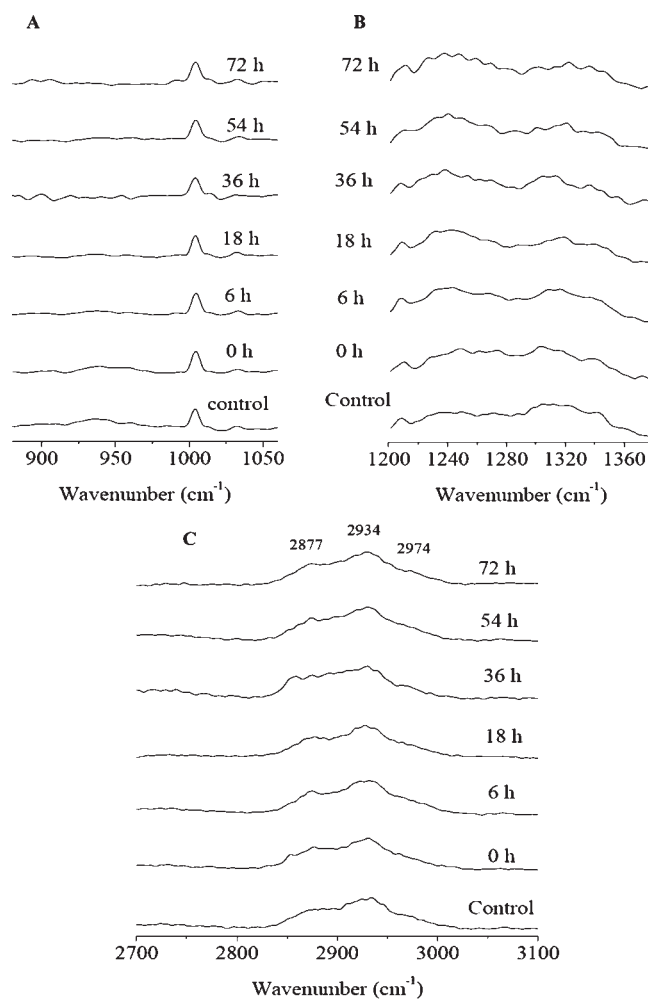


**Figure 4.** Raman spectra of myofibrillar proteins from raw muscle and Cantonese sausage at different processing periods. (A) The wavenumber range of  $890\text{--}1100\text{ cm}^{-1}$ , (B) the amide III ( $1220\text{--}1275\text{ cm}^{-1}$ ), and (C) the wavenumber range of  $2700\text{--}3100\text{ cm}^{-1}$ .

in-plane bending. The amide III band is difficult to interpret by the fact that vibrational spectroscopy of proteins produces a complex pattern of bands in the  $1225\text{--}1350\text{ cm}^{-1}$  range (Figure 4B). This is due to the fact that the characteristic frequency ranges for  $\beta$ -sheet ( $1230\text{--}1245\text{ cm}^{-1}$ ) and random coil ( $1240\text{--}1255\text{ cm}^{-1}$ ) overlap to some extent.<sup>26</sup> Bands near  $1250$  and  $1308\text{ cm}^{-1}$  in the myofibrillar proteins from Cantonese sausage (Figure 4B) are similar to those reported at  $1252$  and  $1304\text{ cm}^{-1}$  for Pacific cod myosin<sup>20</sup> and  $1265$  and  $1304\text{ cm}^{-1}$  for myosin.<sup>14</sup> These two features have been attributed to the  $\alpha$ -helical structures in the globular and fibrous conformations of the myosin head and tail regions, respectively.<sup>14</sup> A slight decreasing intensity except for the 36th hour was observed at the band near  $1308\text{ cm}^{-1}$  during processing of Cantonese sausage (Figure 4B), indicating that the  $\alpha$ -helical structure decreased. The  $\beta$ -sheet structures usually lead to a more intense band near  $1230\text{--}1245\text{ cm}^{-1}$ , while random coil structures appear near  $1250\text{ cm}^{-1}$ . There is a slight intensity increase except for the 36th hour observed near  $1230\text{--}1245\text{ cm}^{-1}$  during the processing of Cantonese sausage (Figure 4B), suggesting that the  $\beta$ -sheet structure increased. Besides, the weaker shoulder band at about  $1232\text{ cm}^{-1}$  was observed during processing except at the 36th hour and control, which was

**Table 2.** Normalized Intensities of the Tryptophan Bands (757 and 1340  $\text{cm}^{-1}$ ), Tyrosyl Doublet (850/830  $\text{cm}^{-1}$ ), CC Band (940  $\text{cm}^{-1}$ ), and CH Band (2934  $\text{cm}^{-1}$ ) of Myofibrillar Proteins from Cantonese Sausage<sup>a</sup>

	$I_{850}/I_{830}$ ( $\text{cm}^{-1}$ )	$I_{940}/I_{1004}$ ( $\text{cm}^{-1}$ )	$I_{757}/I_{1004}$ ( $\text{cm}^{-1}$ )	$I_{1340}/I_{1004}$ ( $\text{cm}^{-1}$ )	$I_{2934}/I_{1004}$ ( $\text{cm}^{-1}$ )
control	1.32 ± 0.16 a	0.50 ± 0.07 a	0.87 ± 0.06 bc	0.38 ± 0.06 a	0.19 ± 0.03 b
0 h	1.27 ± 0.20 a	0.26 ± 0.06 b	0.82 ± 0.12 bc	0.36 ± 0.06 a	0.19 ± 0.02 b
6 h	0.94 ± 0.16 b	0.19 ± 0.04 bc	0.86 ± 0.06 bc	0.30 ± 0.06 ab	0.19 ± 0.03 b
18 h	0.93 ± 0.11 b	0.17 ± 0.05 bc	0.99 ± 0.07 b	0.27 ± 0.04 ab	0.19 ± 0.03 b
36 h	0.87 ± 0.10 b	0.14 ± 0.05 bc	1.29 ± 0.12 a	0.27 ± 0.03 ab	0.25 ± 0.04 a
54 h	0.92 ± 0.11 b	0.18 ± 0.04 bc	0.67 ± 0.11 c	0.22 ± 0.02 b	0.18 ± 0.04 b
72 h	0.85 ± 0.08 b	0.10 ± 0.03 c	0.65 ± 0.12 c	0.24 ± 0.04 b	0.17 ± 0.04 b

<sup>a</sup> Values in a column followed by different letters are significantly different ( $p < 0.05$ ).

considered to be related to the increase in parallel  $\beta$ -sheet content.<sup>20</sup> Raman spectra of myofibrillar proteins at the 36th hour were different to the other periods. It further confirmed the rebuilding process of Cantonese sausage protein during processing. The results from amide III were consistent with data from amide I Raman band.

**Hierarchical Cluster Analysis of Amide III.** A dendrogram of amide III of myofibrillar proteins from raw muscle and Cantonese sausage at different processing periods is shown in Figure 3B. It also could be divided into three clusters, the same as amide I. It was interesting to observe that the control and 72nd hour clustered together first, and then, the 6th and 54th hours clustered. Then, zeroth and 18th hours successively clustered into the group of control and 54th hours, respectively. These discrepancies to amide I might be due to distinct vibrational modes of the polypeptide chain. Amide I vibrational mode involves mainly C=O stretching vibrations and, partly, C–N stretching, C $\alpha$ –C–N bending, and N–H in-plane bending of peptide groups, while amide III mode involves mainly C–N stretching and N–H in-plane bending vibrations of the peptide bond as well as contributions from C $\alpha$ –C stretching and C=O in-plane bending.<sup>11,27</sup>

**C–C Stretching Vibrations.** Another way of looking at the secondary structure is the use of the C–C stretching vibrations in 890–1060  $\text{cm}^{-1}$ . The results showed an intensity decrease trend in the Raman band near 940  $\text{cm}^{-1}$  during processing (Table 2). Gradual loss of  $\alpha$ -helix structure leads to broadening and weakening in the intensity of this band.<sup>15</sup> The changes in the spectrum profile were in agreement with this theory (Figure 4A). However, the obvious shoulder band at 900  $\text{cm}^{-1}$  at the 36th hour was detected. The decline of the 900  $\text{cm}^{-1}$  band intensities suggested that the  $\alpha$ -helices are dissociated to some extent by heat treatment at 40 °C.<sup>26</sup> This indicated the  $\alpha$ -helix increased during 18–36 h. These results were consistent with data from amide I Raman band.

**Tryptophan Residues and Tyrosine (Tyr) Doublet Bands.** Raman bands at 757 and 1340  $\text{cm}^{-1}$  display information about the microenvironment of the tryptophan (Trp) residues. The intensity of the bands near 1340  $\text{cm}^{-1}$  slightly decreased ( $p < 0.05$ ) during Cantonese sausage processing (Table 2), which perhaps indicated the exposure of Trp residues. Similar findings were reported by Bouraoui, Nakai, and Li-Chan.<sup>20</sup> However, the  $I_{757}/I_{1004}$  showed no significant difference ( $p > 0.05$ ) during 18 h, then increased to the maximum of 1.29 at the 36th hour, and decreased during the final phase of processing. It should be noted that the overlap of Trp band at 757  $\text{cm}^{-1}$  with that at 755  $\text{cm}^{-1}$  was assigned to aliphatic residues.<sup>28</sup>

The intensity ratio  $I_{850}/I_{830}$  was determined for the Tyr doublet at 830 and 850  $\text{cm}^{-1}$ . It has been suggested by Yu, Jo,

and O'Shea<sup>29</sup> that the ratio of the Tyr ring vibrations at 850 and 830  $\text{cm}^{-1}$  ( $R_{\text{Tyr}}$ ) reflects “buried” and “exposed” Tyr groups.  $R_{\text{Tyr}} \geq 1$  in the myosin Raman spectrum is indicative of Tyr residues exposed on the protein surface, which interact with water molecules as a hydrogen bond donor and acceptor. If  $R_{\text{Tyr}}$  falls between 0.7 and 1.0, the Tyr residues are considered “buried”. The intensity ratios  $I_{850}/I_{830}$  of control and zeroth hour were 1.32 and 1.27, respectively, suggesting that the Tyr residues of these samples were mainly exposed and able to participate in the formation of moderate or weak hydrogen bonds. During the processing of Cantonese sausage, the intensity ratios  $I_{850}/I_{830}$  decreased significantly ( $p < 0.05$ ) to 0.85–0.94, suggesting that some Tyr residues became buried in a more hydrophobic environment. This result was in agreement with the report of Ogawa et al.,<sup>30</sup> who also found the tyrosyl doublet ratio had showed a decrease as an effect of heat process on lemon sole (*Microstomus kitt*) actomyosin. In the present work, the Tyr residues were less exposed to the surface during processing, probably because of intermolecular interactions during protein network formation.<sup>31</sup> However, Herrero et al.<sup>9</sup> have reported that the Tyr residues are buried in a hydrophobic environment independently of thermal treatment and NaCl content.

**Aliphatic C–H Stretching Vibrations.** Raman spectra in the wavenumber range of 2800–3000  $\text{cm}^{-1}$  are assigned to C–H stretching bands. Myofibrillar proteins of control showed a distinct peak at 2885  $\text{cm}^{-1}$  attributable to the CH<sub>2</sub> asymmetric stretch, along with a discernible shoulder at 2934  $\text{cm}^{-1}$  arising from the CH<sub>3</sub> symmetric and/or CH<sub>2</sub> asymmetric stretch.<sup>30</sup> During processing, these two peaks shifted slightly toward lower frequencies of 2930 and 2874  $\text{cm}^{-1}$ , and a small shoulder appeared at 2860  $\text{cm}^{-1}$  due to CH<sub>2</sub> symmetric stretch (Figure 4C). Similar findings have been reported by Ogawa et al.<sup>30</sup> Careche and Li-Chan<sup>12</sup> have reported that a shift to higher wavenumbers in the C–H stretching band at 2933  $\text{cm}^{-1}$  is observed after frozen denaturation of cod myosin, and it stems from enhanced exposure of the aliphatic residues to the aqueous environment. Ogawa et al.<sup>30</sup> have pointed out that the observed peak shift toward lower frequencies in the 2855–2940  $\text{cm}^{-1}$  region suggests that the microenvironment of aliphatic side chains is changed upon heating, although it is not confirmed whether the changes can be interpreted as enhanced exposure.

The intensity of the band near 2930  $\text{cm}^{-1}$  kept constantly until the 36th hour, then increasing to the maximum of 0.25, and thereafter decreasing at the rest stage. In addition, an increase of the  $\beta$ -sheet structure during 36–72 h could be observed (Table 1). It is well-known that the  $\beta$ -sheet structure is comprised of characteristic hydrogen bonds involving the polypeptide backbone. Therefore, Herrero et al.<sup>9</sup> have assumed that

thermal treatment and salting induce mainly rearrangement of hydrogen bonds resulting in  $\beta$ -sheet formation. Cofrades and Jiménez-Colmenero<sup>3</sup> have found that the molecular associations involved in gel network formation during the elaboration in frankfurter comprise  $\beta$ -sheet hydrogen-bonding and hydrophobic interactions, which are equally involved in protein denaturation and aggregation. Therefore, changes in the intensity of the band near  $2930\text{ cm}^{-1}$  during processing might be due to salting and heat treatment. These results further confirmed the rebuilding behavior of myofibrillar proteins during final stage.

In conclusion, this investigation showed that Raman spectroscopy was a useful technique to evaluate the protein structural changes during Cantonese sausage processing. Decreases in the  $\alpha$ -helix structure accompanied by increases in  $\beta$ -sheets were observed during 0–18 and 36–72 h. The discrepancies at the 36th hour indicated that a rebuilding process of secondary structures occurred at the rest stage. Analysis of amide III and C–C stretching vibrations in  $890\text{--}1060\text{ cm}^{-1}$  confirmed it. The hierarchical cluster analysis results of amides I and III and the wavenumber range of  $2855\text{--}2940\text{ cm}^{-1}$  further confirmed this rebuilding process. Changes in a doublet near  $850$  and  $830\text{ cm}^{-1}$  suggested that some Tyr residues became buried in a more hydrophobic environment. Results from aliphatic C–H stretching vibrations showed that the microenvironment of aliphatic side chains might be changed during final stage.

## AUTHOR INFORMATION

### Corresponding Author

\*Tel/Fax: +86 20 87113914. E-mail: femmzhao@scut.edu.cn.

### Funding Sources

We are grateful to the Science and Technology Program of Guangdong Province (Nos. 2010B080701103 and 2009A02010-1002) and National Special Funds for Scientific Research on Public Causes of Agriculture (No. 200903012) for their financial support.

## REFERENCES

- (1) Tornberg, E. Effects of heat on meat proteins—Implications on structure and quality of meat products. *Meat Sci.* **2005**, *70*, 493–508.
- (2) Li, C. T.; Wick, M. Improvement of the physicochemical properties of pale soft and exudative (PSE) pork meat products with an extract from mechanically deboned turkey meat (MDTM). *Meat Sci.* **2001**, *58*, 189–195.
- (3) Cofrades, S.; Jiménez-Colmenero, F. Protein molecular interactions involved in the formation of frankfurters: Effect of fat level and heating rate. *Meat Sci.* **1998**, *49*, 411–423.
- (4) Ho, C. Y.; Stromer, M. H.; Robson, R. M. Effect of electrical stimulation on postmortem titin, nebulin, desmin, and troponin-T degradation and ultrastructural changes in bovine longissimus muscle. *J. Anim. Sci.* **1996**, *74*, 1563–1575.
- (5) Morzel, M.; Chambon, C.; Hamelin, M.; Santé-Lhoutellier, V.; Sayd, T.; Monin, G. Proteome changes during pork meat ageing following use of two different pre-slaughter handling procedures. *Meat Sci.* **2004**, *67*, 689–696.
- (6) Xiong, Y. O. L. Thermally Induced Interactions and Gelation of Combined Myofibrillar Protein from White and Red Broiler Muscles. *J. Food Sci.* **1992**, *57*, 581–585.
- (7) Bertram, H. C.; Kohler, A.; Böcker, U.; Ofstad, R.; Andersen, H. J. Heat-Induced Changes in Myofibrillar Protein Structures and Myowater of Two Pork Qualities. A Combined FT-IR Spectroscopy and Low-Field NMR Relaxometry Study. *J. Agric. Food Chem.* **2006**, *54*, 1740–1746.
- (8) Wu, Z.; Bertram, H. C.; Kohler, A.; Böcker, U.; Ofstad, R.; Andersen, H. J. Influence of Aging and Salting on Protein Secondary Structures and Water Distribution in Uncooked and Cooked Pork. A Combined FT-IR Microspectroscopy and  $^1\text{H}$  NMR Relaxometry Study. *J. Agric. Food Chem.* **2006**, *54*, 8589–8597.
- (9) Herrero, A. M.; Carmona, P.; López-López, I.; Jiménez-Colmenero, F. Raman Spectroscopic Evaluation of Meat Batter Structural Changes Induced by Thermal Treatment and Salt Addition. *J. Agric. Food Chem.* **2008**, *56*, 7119–7124.
- (10) Pelton, J. T.; McLean, L. R. Spectroscopic methods for analysis of protein secondary structure. *Anal. Biochem.* **2000**, *277*, 167–176.
- (11) Herrero, A. M. Raman spectroscopy for monitoring protein structure in muscle food systems. *Crit. Rev. Food Sci. Nutr.* **2008a**, *48*, 512–523.
- (12) Li-Chan, E. The applications of Raman spectroscopy in food science. *Trends Food Sci. Technol.* **1996**, *7*, 361–370.
- (13) Brøndum, J.; Byrne, D. V.; Bak, L. S.; Bertelsen, G.; Engelsen, S. B. Warmed-over flavour in porcine meat—A combined spectroscopic, sensory and chemometric study. *Meat Sci.* **2000**, *54*, 83–95.
- (14) Carew, E.; Asher, I.; Stanley, H. Laser raman spectroscopy—New probe of myosin substructure. *Science* **1975**, *188*, 933–936.
- (15) Barrett, T. W.; Peticolas, W. L.; Robson, R. M. Laser Raman Light-Scattering Observations of Conformational Changes in Myosin Induced by Inorganic Salts. *Biophys. J.* **1978**, *23*, 349–358.
- (16) Martinaud, A.; Mercier, Y.; Marinova, P.; Tassy, C.; Gatellier, P.; Renner, M. Comparison of Oxidative Processes on Myofibrillar Proteins from Beef during Maturation and by Different Model Oxidation Systems. *J. Agric. Food Chem.* **1997**, *45*, 2481–2487.
- (17) Flores, M.; Barat, J. M.; Aristoy, M. C.; Peris, M. M.; Grau, R.; Toldrá, F. Accelerated processing of dry-cured ham. Part 2. Influence of brine thawing/salting operation on proteolysis and sensory acceptability. *Meat Sci.* **2006**, *72*, 766–772.
- (18) Susi, H.; Byler, D. M. Fourier deconvolution of the amide I Raman band of proteins as related to conformation. *Appl. Spectrosc.* **1988**, *42*, 819–826.
- (19) Beattie, R. J.; Bell, S. J.; Farmer, L. J.; Moss, B. W.; Patterson, D. Preliminary investigation of the application of Raman spectroscopy to the prediction of the sensory quality of beef silverside. *Meat Sci.* **2004**, *66*, 903–913.
- (20) Bouraoui, M.; Nakai, S.; Li-Chan, E. In situ investigation of protein structure in Pacific whiting surimi and gels using Raman spectroscopy. *Food Res. Int.* **1997**, *30*, 65–72.
- (21) Sun, W.; Zhao, H.; Zhao, Q.; Zhao, M.; Yang, B.; Wu, N.; Qian, Y. Structural characteristics of peptides extracted from Cantonese sausage during drying and their antioxidant activities. *Innovative Food Sci. Emerging Technol.* **2009**, *10*, 558–563.
- (22) Panyam, D.; Kilara, A. Enhancing the functionality of food proteins by enzymatic modification. *Trends Food Sci. Technol.* **1996**, *7*, 120–125.
- (23) Kristinsson, H. G.; Rasco, B. A. Biochemical and Functional Properties of Atlantic Salmon (*Salmo salar*) Muscle Proteins Hydrolyzed with Various Alkaline Proteases. *J. Agric. Food Chem.* **2000**, *48*, 657–666.
- (24) Sun, W. Z.; Cui, C.; Zhao, M. M.; Zhao, Q. Z.; Yang, B. Effects of composition and oxidation of proteins on their solubility, aggregation and proteolytic susceptibility during processing of Cantonese sausage. *Food Chem.* **2011**, *124*, 336–341.
- (25) da Silva Torres, E. A. F.; Garbelotti, M. L.; Moita Neto, J. M. The application of hierarchical clusters analysis to the study of the composition of foods. *Food Chem.* **2006**, *99*, 622–629.
- (26) Herrero, A. M. Raman spectroscopy a promising technique for quality assessment of meat and fish: A review. *Food Chem.* **2008b**, *107*, 1642–1651.
- (27) Krimm, S.; Bandekar, J. Vibrational spectroscopy and conformation of peptides, polypeptides, and proteins. *Adv. Protein Chem.* **1986**, *38*, 181–364.
- (28) Careche, M.; Li-Chan, E. C. Y. Structural Changes in Cod Myosin after Modification with Formaldehyde or Frozen Storage. *J. Food Sci.* **1997**, *62*, 717–723.

(29) Yu, N. T.; Jo, B. H.; O'Shea, D. C. Laser Raman scattering of cobramine B, a basic protein from cobra venom. *Arch. Biochem. Biophys.* **1973**, *156*, 71–76.

(30) Ogawa, M.; Nakamura, S.; Horimoto, Y.; An, H.; Tsuchiya, T.; Nakai, S. Raman Spectroscopic Study of Changes in Fish Actomyosin during Setting. *J. Agric. Food Chem.* **1999**, *47*, 3309–3318.

(31) Nonaka, M.; Li-Chan, E.; Nakai, S. Raman spectroscopic study of thermally induced gelation of whey proteins. *J. Agric. Food Chem.* **1993**, *41*, 1176–1181.

(32) Iconomidou, V. A.; Chryssikos, D. G.; Gionis, V.; Pavlidis, M. A.; Paipetis, A.; Hamodrakas, S. J. Secondary Structure of Chorion Proteins of the Teleostean Fish *Dentex dentex* by ATR FT-IR and FT-Raman Spectroscopy. *J. Struct. Biol.* **2000**, *132*, 112–122.